J. Fluid Mech. (1977), *vol.* 81, *part* 4, *pp.* 701–717
Printed in Great Britain

Photogrammetry of spherical shocks reflected from real and ideal surfaces

By J. M. DEWEY, D. J. McMILLIN AND D. F. CLASSEN
University of Victoria, P.O. Box 1700, Victoria, B.C., Canada

(Received 30 July 1976)

A photogrammetrical technique has been used to study the interaction of two identical explosively produced spherical shock waves and to compare this interaction with the reflexion of one of the spherical shocks from the ground. It is postulated that there was no energy loss in the interaction of the two shock waves and that the interaction therefore simulated the reflexion of a spherical shock from an ideal non-energy-absorbing surface. The 'ideal' reflexions were compared with real reflexions from two types of ground surface: one smooth and the other rough. Experiments were carried out with the centres of the spherical shocks at two separations so that observations could be made of the interaction of shocks of different strength. Significant differences were shown to exist in both the strengths of the Mach shocks and in the triple-point trajectories over the different surfaces. The results are intended to aid in the evaluation of computer codes being developed to simulate spherical-shock reflexions from real surfaces.

1. Introduction

When a centred explosion is initiated above the ground, the primary spherical blast wave is reflected, and, at an incidence angle of approximately 45°, the so-called regular reflexion changes to irregular or Mach reflexion. This is characterized by the reflected and incident shocks combining to form a single shock known as the Mach stem. In a vertical plane containing the centre of the explosion, the point at which the incident, reflected and Mach-stem shocks meet is called the triple point. As the Mach stem travels across the reflecting surface the triple point rises along a curved trajectory.

The physical properties of the Mach-stem blast wave and the trajectory of the triple point depend mainly on the energy yield of the explosive charge, the height of burst of the charge above the ground and the nature of the ground surface. As the blast wave interacts with the ground, some energy will be absorbed and appear as seismic disturbances, and a crater may be produced if the explosion is close enough to the ground. As the Mach-stem blast wave moves across the ground surface there will be a continuous transfer of energy between the air and the ground and a redistribution of energy within the blast wave due to ground roughness. Little is known qualitatively or quantitatively about the transfer of energy from a blast wave to the ground or the redistribution of energy within a blast wave as it passes over the ground surface. The exact point of transition between regular and Mach reflexion is not known, even for a plane shock reflecting from a rigid smooth surface (Henderson & Lozzi 1975).

Because of the complexity of the phenomena associated with a centred explosion followed by regular and irregular blast reflexion at an arbitrary surface, an analytical

description of these phenomena is not feasible. Therefore a number of computer codes are being developed for studying this type of problem (Amsden & Hirt 1973; Needham 1973, private communication). Reasonable numerical solutions have been obtained for free-field centred explosions (Brode 1959), but difficulties have been encountered in handling shock reflexions because the mechanism of energy transfer between the air and the solid surface, and the subsequent boundary-layer effects, are not understood. It is hoped that the results of the experiments described here will be of value in improving computer techniques for the solution of blast-reflexion problems.

A useful starting point for this investigation would appear to be the study of the perfect reflexion of a spherical shock at a boundary which would cause no energy loss or redistribution. If two identical explosive charges a certain distance apart are detonated simultaneously, the two resulting identical spherical blast waves will interact along a plane midway between the two charge centres. Since there will be no energy loss in this interaction it is postulated that this will simulate an ideal spherical-shock reflexion, corresponding to the classical analytical approach in which a rigid plane is simulated by the use of an image source. The properties of the Mach-stem blast wave above and below the ideal reflecting plane may then be compared with those produced by a reflexion from a real ground surface.

Photogrammetrical studies have been made of four such experiments using, in each case, two identical simultaneously detonated spherical explosive charges. In each experiment the charges were suspended one above the other such that the distance between them was equal to twice the height of the lower charge above the ground. Two different charge separations were used over two different types of ground surface. Figure 1 illustrates the positions of the explosive charges relative to the ground, and the expected shock wave patterns at various times after the simultaneous detonation of the charges.

The specific project reported here involved the photography, against a suitably prepared background, of the primary shock from the lower charge and the Mach-stem shocks produced above the ground and below the ideal reflecting plane between the charges. The objective was to measure the space–time trajectories of these three shocks from the resulting photographic records and thus calculate the shock speed in each case. The shock Mach number could then be used to determine the physical properties of the air immediately behind the shock. In addition, measurements could be made of the trajectories of the triple point above the ground and below the ideal reflecting plane.

2. Experimental procedure

Explosive charges

The four experiments described here were carried out at the Defence Research Establishment Suffield in Alberta, Canada, during 1973. Each experiment consisted of the simultaneous detonation of two spherical charges of cast pentolite. Pentolite is a mixture of 50 % trinitrotoluene and 50 % pentaerythritol tetranitrate, with a detonation velocity of 7450 m s^{-1}. The eight charges were approximately equal in mass, the average being 489·9 kg, and were cast by Canadian Arsenal Limited of Quebec.

In each experiment the two charges were suspended, one above the other, from the midpoint of a cable stretched between two towers 61 m high and 122 m apart. In two of the experiments the centre of the lower charge was at a nominal height of 4·6 m

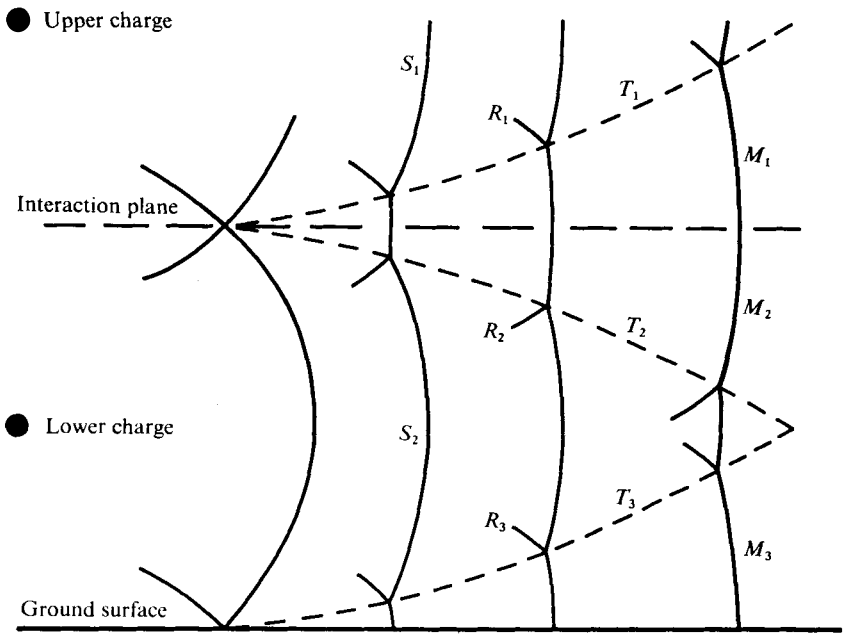

FIGURE 1. Positions of the spherical charges relative to the ground and the interaction plane. The solid lines show the expected positions of shock fronts at four times after detonation. S_1 and S_2 are the spherical shocks from the upper and lower charges, respectively, R_1, R_2 and R_3 are the reflected shocks, M_1, M_2 and M_3 are the Mach-stem shocks above and below the interaction plane and above the ground surface, and the broken lines, T_1, T_2 and T_3, are the triple-point trajectories.

above the ground and the second charge at an additional altitude of twice that distance, namely 9·2 m. In the other two experiments the corresponding distances were 7·6 and 15·2 m respectively. In this way the lower charge in each experiment was equidistant from the ground and the horizontal interaction plane mid-way between the two charges.

Photography

The high-speed cameras used to record the shock waves produced by the simultaneous explosions were mounted 183 m due south of ground zero, where ground zero is defined as the point on the ground vertically beneath the two charges. Photography of the shock fronts was made possible by viewing the shocks against a 15 m high backdrop. This backdrop began at a point 122 m beyond the charges, as viewed from the camera position, and extended for a distance of 100 m, approximately parallel to the film plane of the cameras. The backdrop consisted of ten 9 m wide canvas sheets painted with black and white stripes.

To observe the Mach stem close to the ground a camera was placed at a minimum practical height of 1 m. The Mach stem beneath the interaction plane between the charges was photographed by two cameras mounted at the approximate height of that plane, namely 15 or 9 m depending on the charge separation being used. Photographs taken with an upper-level camera are shown in figures 2(*a*) and (*b*) (plate 1). The photograph in figure 2(*b*) was taken approximately 25 ms after the simultaneous detonation of the charges.

Three sets of fiducial markers were placed in the fields of view of the cameras. The first set was placed along the top edge of the backdrop, and these can be seen in figures 2(*a*) and (*b*). The second set of markers was placed at ground level, at three positions on a circle whose diameter was the line joining the camera position to ground zero. It will be shown later that this circle is the ground-level trajectory of the point on a shock front seen from the camera position. Therefore, when a shock is observed to traverse one of the markers in this set, its exact position is known without making any geometrical corrections. The third set of markers was placed at ground level in the immediate foreground of the ground-level camera. Other objects in the fields of view of the cameras whose positions were known, such as pressure gauges, were also used as fiducial markers.

Camera orientation and position

The optical axis of each camera was defined by an azimuthal and an elevation angle. These orientation angles were not measured at the time of the experiment, and in addition the camera positions relative to the charges were measured only approximately. The orientations and positions of the cameras were therefore determined from the photographs of the fiducial markers.

The orientation angles were found by considering a triangle defined by the frame centre and the images of two fiducial markers in the projected film plane. If correct orientation angles are used, the ratio of the lengths of two sides of the triangle and the angle between these sides remain constant under transformation from the projected measurement plane to the object plane. An iteration procedure was used to match the similarities of the triangles. The camera orientation was considered to have been determined when successive iterations differed by less than 0·001°. So that the orientation process would not be particularly sensitive to small errors in camera position, orientation reference points were chosen in a plane which differed minimally from the object plane.

The camera position was obtained by using two secondary fiducial points chosen as far as possible from the object plane. The lateral and elevation co-ordinates of each camera were determined by ensuring that the image of one of these secondary fiducial points, when transformed to the object plane, coincided with its position calculated directly from the surveyed marker position. The axial co-ordinate of each camera was determined by ensuring that the distance between the images of the two secondary fiducial points, transformed to the object plane, was the same as the distance calculated from the surveyed marker positions. The camera position was considered determined when successive iterations differed by less than 3 cm in each direction.

The camera used to photograph the Mach stem above the ground was a Fastax WF3T† 16 mm camera operated at a nominal speed of 4000 frames/s. The cameras used at the elevated position to photograph the Mach stem beneath the ideal reflecting surface were a 35 mm Fastax WF5 and a 16 mm Fastax WF3T, operating at nominal speeds of 3000 and 4000 frames/s respectively. Timing marks were imposed on all the films at 1 ms intervals and, in addition, a zero time mark coincident with the detonation pulse to the charges was recorded on each film. In this way, the exact time at which each picture was taken, relative to the detonation pulse, could be calculated.

† Red Lake Laboratories Inc., Santa Clara, California.

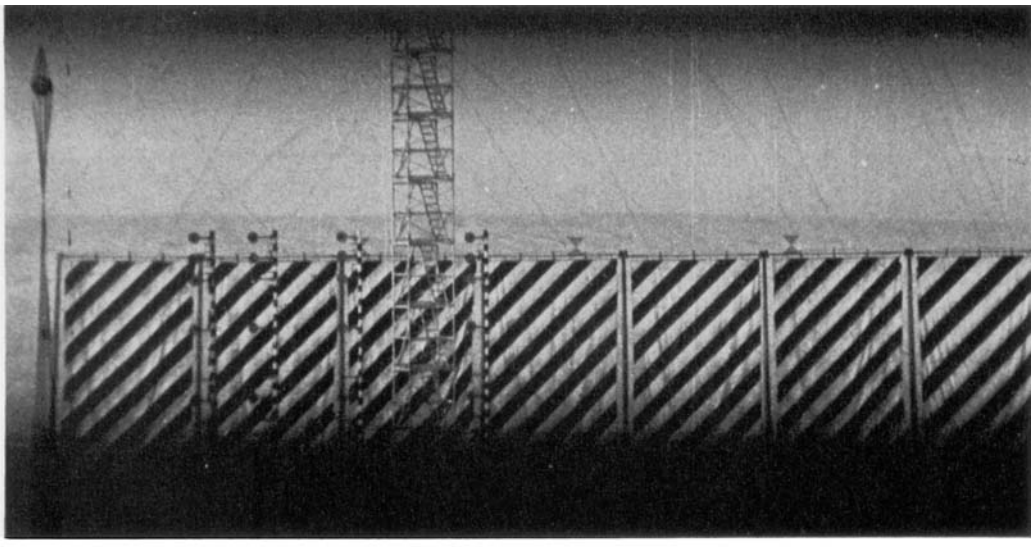

(*a*)

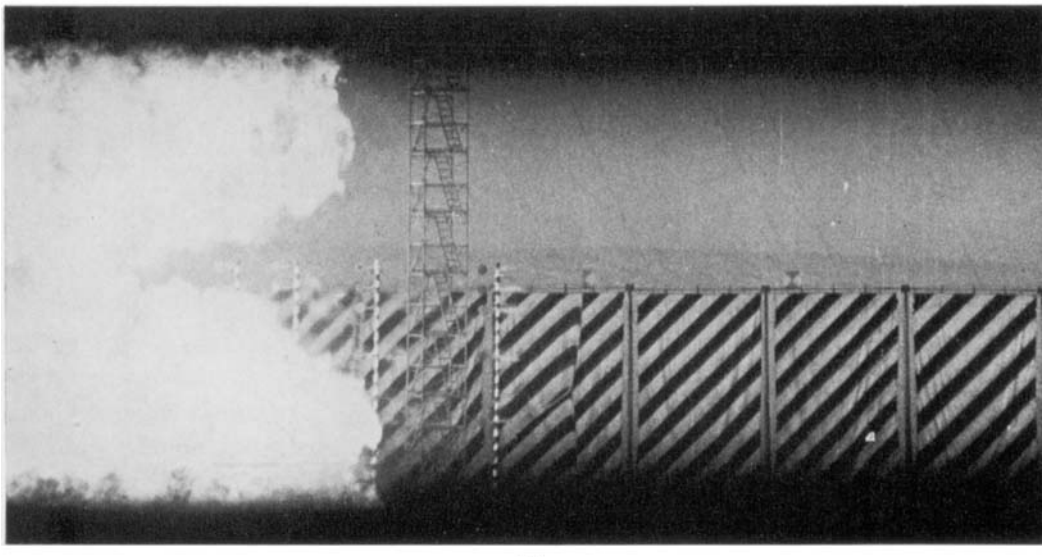

(*b*)

FIGURE 2. (*a*) Photograph taken with a camera at a height of 17·4 m before the charges were detonated. The two charges, suspended in nylon-webbing slings, can be seen on the left-hand side. The charges are at nominal heights of 7·6 and 22·8 m above the ground. The top of the striped background is just above the ideal reflecting surface viewed from this position. A section of one of the towers used to support the charges can be seen in the centre of the picture. Three of the fiducial markers are on the top of the backdrop. A number of round pressure-transducer mounts, supported on four black-and-white poles, are visible in the photograph. The transducer positions were accurately surveyed and were used as additional fiducial markers. (*b*) Photograph taken approximately 25 ms after the simultaneous detonation of the charges. The Mach stem below the ideal reflecting surface, the reflected shock and the primary shock from the lower charge can be seen against the central backdrop panel.

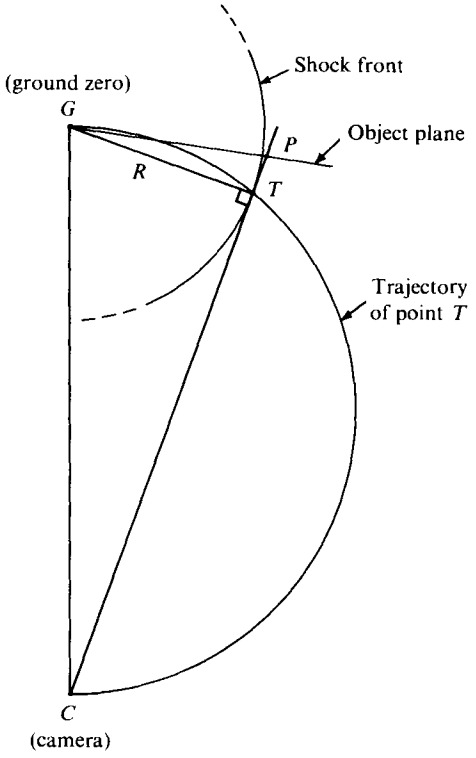

FIGURE 3. A plan view of the locus of the observed point T on a spherical shock front. The line of sight from the camera is tangential to the shock sphere at T. R is the shock radius. The locus of T is a circle with the line joining the camera to the charge as diameter.

3. Method of analysis

Geometrical transformations

In order to determine the actual position of a shock front from measurements of its image in a photograph, a number of geometrical corrections were required. First, a transformation was made from the projected image or record plane, in which the measurements were made, to an object plane defined as parallel to the record and film planes and containing ground zero. To make this transformation it was assumed that the optics of the camera and the projection system had cylindrical symmetry such that both the film and the record plane were perpendicular to a single optical axis which intersected both planes at the frame centre.

A further geometrical transformation was required because the image of a three-dimensional shock surface seen against a background defines only the line of sight tangential to the shock front. To obtain the position of a shock front a unique geometrical transformation was necessary for each data point obtained from each photograph. This transformation is illustrated in plan view in figure 3. The axis of cylindrical symmetry of the shock intersects the plane of the figure at G. The camera is at C. The line of sight from the camera to the shock is tangential to the shock front at T and intersects the object plane at P. The position of P is calculated from its image in the record plane, and this determines the line of sight CT. The radius of a shock front is the

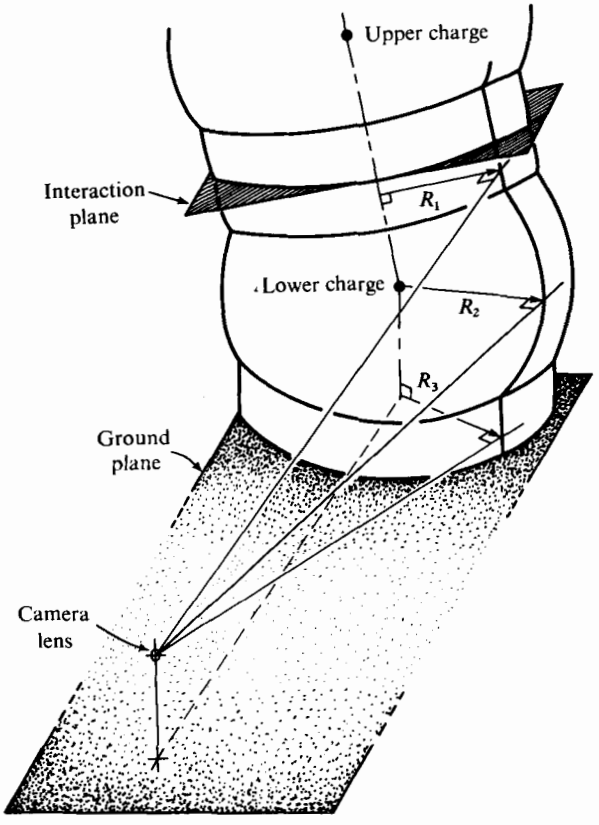

FIGURE 4. A visualization of spherical shocks and Mach-stem shocks produced by a simultaneous double explosion above the ground. The shock radii R_1, R_2 and R_3 are defined by the lines of sight from the camera tangential to the shock surfaces. The line joining the two charge centres was not assumed to be vertical and this lack of symmetry has been exaggerated in the diagram.

distance from this line to the axis for a cylindrically symmetric shock or to the centre for a spherical shock. In the case of a spherical shock all tangent points T lie on a sphere with the line joining the charge centre to the camera as diameter. In the case of a cylindrical Mach stem, T lies on a cylinder whose axis is parallel to the axis of symmetry of the shock, and which has the latter axis and a parallel axis through the camera as diametrically opposite generators.

The shock surfaces, tangent lines of sight and shock radii for the experiments described here are illustrated in figure 4. It was not assumed that the charges were exactly above each other, and this lack of symmetry is exaggerated in the figure. The axis of symmetry for the Mach stems above and below the ideal reflecting surface was taken as the line joining the two charges. The axis of symmetry for the Mach stem at the ground was taken as the vertical through the centre of the lower charge. It was assumed that the primary shocks were spherical and that the Mach stems were cylindrical close to the reflecting surfaces.

Determination of shock velocity

Application of these geometrical transformations to the measurements from the films gave a sequence of radial positions and times for each shock. On the average, a hundred such data pairs were obtained for each shock, with a minimum of 20 and a maximum of 176. These data were analysed by least-squares fitting to an equation of the form

$$R = A + Bt + C\ln(1+t) + D[\ln(1+t)]^{\frac{1}{2}},$$

where R is the radius of the shock, t the time measured after the detonation pulse and A, B, C and D are the fitted coefficients. The data were weighted inversely with the square of the observed radius so as to obtain a fit with a constant percentage error throughout the range of input data. This *ad hoc* equation has been found valuable for describing a variety of monotonically decaying shocks (Dewey 1964, 1971). It satisfies two appropriate boundary conditions, namely that at $t = 0$ the shock radius may have a finite value and that as $t \to \infty$ the shock velocity asymptotically approaches a constant value, which might be expected to be the ambient velocity of sound. This equation may be differentiated with respect to time to obtain the shock-front velocity at any point. The shock velocity was expressed as a Mach number relative to the ambient sound speed.

Shock strength

The strength of a shock wave is normally quoted in terms of the pressure or density ratio across the shock discontinuity. Such ratios were determined for all shocks by calculating the shock Mach number, in the manner described in the previous section, and substituting this value into the well-known extensions of the Rankine–Hugoniot equation, namely

$$\frac{P_s}{P_a} = \frac{2\gamma M^2 - (\gamma - 1)}{\gamma + 1}, \quad \frac{\rho_s}{\rho_a} = \frac{(\gamma+1)M^2}{(\gamma-1)M^2 + 2},$$

where P_s and ρ_s are respectively the pressure and density immediately behind the shock, P_a and ρ_a are the ambient values in front of the shock, M is the Mach speed of the shock and γ the ratio of specific heats. For the relatively weak shocks studied in these experiments, it was assumed that real-gas effects could be ignored, and γ for air was set equal to 1·4. The highest shock velocity measured in any of the experiments was Mach 2·4.

Scaling

The trajectory of an explosively produced shock front is determined both by the amount of energy released from the charge and by the ambient conditions of the gas through which the shock is passing. In order to compare the properties of blast waves from different explosions it is necessary to scale measurements to a standard charge mass in standard atmospheric conditions.

The results given in this paper were scaled to be equivalent to those which would be expected for a 1 kg charge detonated at sea level in dry air at 15 °C. This was achieved by scaling distances by a factor S^{-1}, where

$$S = \left(\frac{W}{W_0}\frac{P_0}{P_a}\right)^{\frac{1}{3}},$$

and times by a factor $c_a(c_0 S)^{-1}$, where W is the charge mass, W_0 a standard charge mass (arbitrarily chosen as 1 kg), P_a the ambient atmospheric pressure, P_0 a standard

Experiment	Nominal height (m)	Actual height (m)	'Ideal' distance (m)	Average scaled height (m)	Ground surface
1	7·6	7·45	7·60	0·93	Smooth
2	4·6	4·63	4·61	0·57	Smooth
3	4·6	4·55	4·64	0·57	Rough
4	7·6	7·31	7·64	0·93	Rough

TABLE 1

atmospheric pressure (101·3 kPa), c_a the ambient velocity of sound and c_0 the speed of sound in dry air at 15 °C (340·29 m s^{-1}). The pressure, density and temperature within the blast wave, expressed as ratios to the ambient values, and the particle velocity, expressed as the ratio to the ambient sound speed, are invariant under this scaling transformation. The validity of this method of scaling has been illustrated previously (Dewey 1964, 1971).

4. Experimental results

Charge configuration

Four experiments were carried out in the order shown in table 1. The nominal height was the planned distance of the centre of the lower charge from both the ground and the ideal reflecting surface. The actual heights above the ground and distances from the ideal surface are also shown. In each experiment the actual height and 'ideal' distance were averaged and scaled by the factor S^{-1} described above. Fortuitously, the average scaled heights were identical for the two experiments in each pair. It would have been impractical to attempt to achieve this under field conditions, as to do so would have entailed in each experiment a careful adjustment of the two charge positions according to the ambient conditions at the time of the experiment.

Nature of ground surface

The ground surface for experiments 1 and 2 was the natural hard-packed smooth prairie soil, which is a light sandy loam. In these two experiments the ground surface was smooth to within 3 or 4 cm out to a distance of 70 m from ground zero. For experiments 3 and 4 the ground surface was furrowed in a circular pattern, centred on ground zero, to a distance of 70 m from ground zero. The average distance between furrows and the average depth of the furrows was 35·5 cm. In areas which could not be furrowed, sand-bags were used to simulate the furrow pattern as closely as possible.

Shock-front photographs

In each experiment good sequences of photographs were obtained of the Mach stems above the ground and below the ideal reflecting plane and of the primary shock wave from the lower charge. The films were analysed by projecting each frame at a magnification of approximately 30:1, and the position of each shock was measured using an x–y digitizer. Figure 5 shows tracings of some of the shocks seen in the film taken by the ground-level camera in the first experiment. Some of the numbers of the film frames

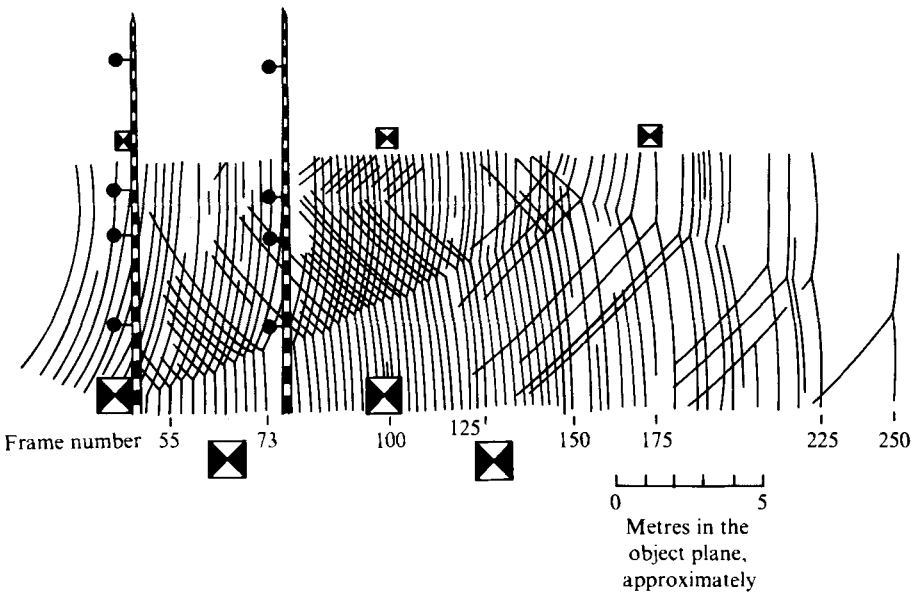

FIGURE 5. Tracings of the primary shock from the lower charge and the Mach stem above the ground as recorded by a camera at a height of 1 m in experiment 1. The number of the film frame is given for some of the tracings. Neither the frame time nor the distance scales are linear. The patterned squares are fiducial markers. The round pressure-gauge holders mounted on vertical poles were accurately surveyed and used as additional fiducial markers.

from which the tracings were made are given, where frame 0 corresponds to the detonation time. It must be stressed that exact radius and time measurements cannot be made directly from this figure since neither the space nor the time scale is linear.

For each of the four experiments radius *vs.* time measurements were made of the primary shock from the lower charge, of the Mach stem produced by the lower charge along the ground surface, and of the Mach stem produced by the lower charge beneath the ideal reflecting plane. The measurements of the radii of the Mach stems were made at an average height of approximately 0·5 m above the ground and at an average distance of approximately 0·2 m below the interaction plane. In experiment 3 it was also possible to measure the trajectory of the Mach stem produced by the upper charge just above the ideal reflecting surface.

In experiments 2 and 3, which used the smaller charge separation, the primary shock from the lower charge could be observed for a distance of approximately 3 m only. As a result no satisfactory analysis of the primary shock trajectory could be made for these two experiments, although a value of the average shock velocity was obtained over the short distance for which measurements were possible.

There was some evidence from the photographs that the Mach-stem shocks were spherical, centred approximately on ground zero or the corresponding point in the interaction plane. Two analyses of the Mach-stem shock trajectories were therefore carried out, one assuming cylindrical symmetry and the other spherical symmetry. No difference could be detected between the results of the two methods of analysis, although this might not have been the case had the measurements not all been made as close as possible to the reflecting surfaces.

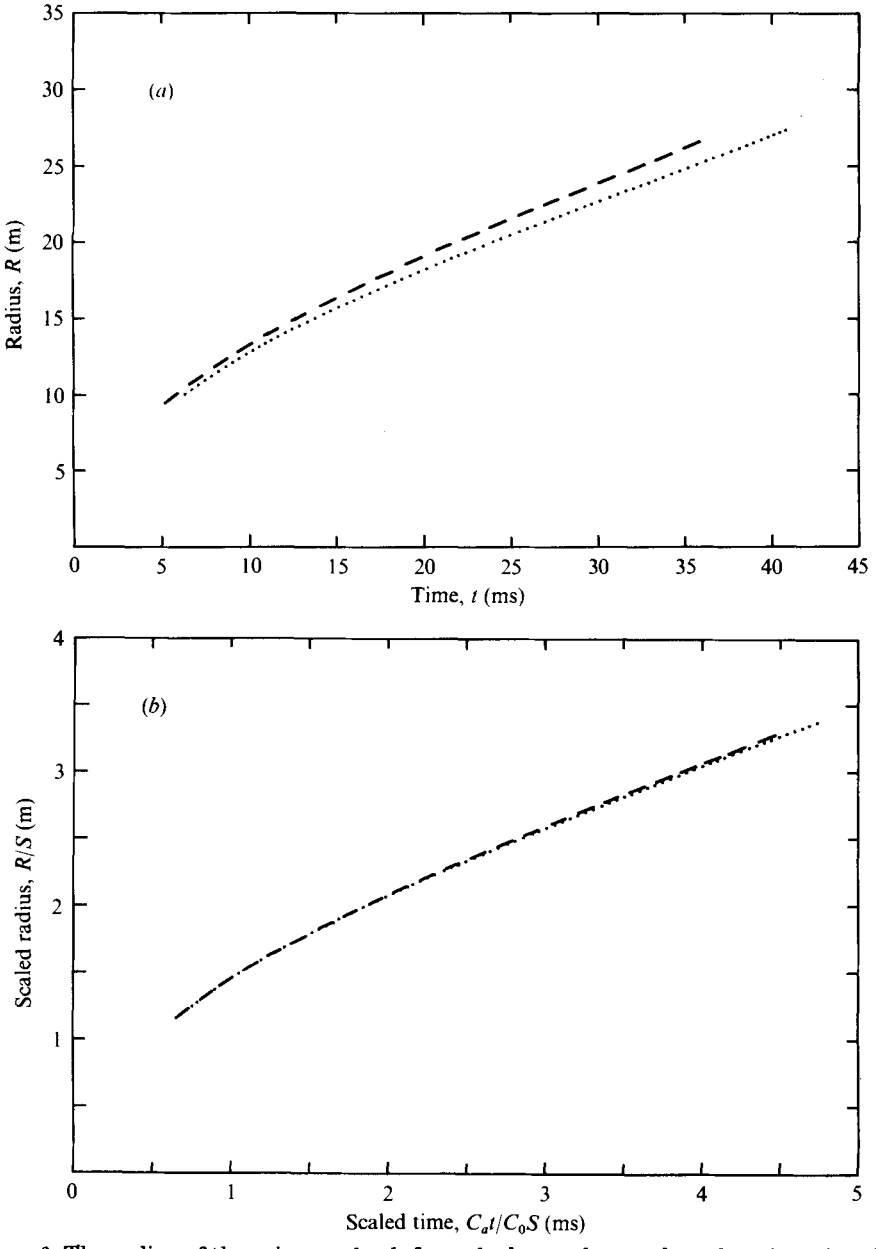

FIGURE 6. The radius of the primary shock from the lower charge plotted against time for experiments 1 and 4, which were carried out under significantly different ambient conditions. – – –, experiment 1; ····· experiment 4. (*a*) Observed data. (*b*) Scaled data.

Shock trajectories

The significance of and necessity for scaling the measured distances and times before comparing results from experiments carried out under different ambient conditions are illustrated in figures 6(*a*) and (*b*). Figure 6(*a*) shows the unscaled trajectories of the primary shock fronts from the lower charges in experiments 1 and 4. Experiment 1 was carried out at an ambient temperature of 19·7 °C, an atmospheric pressure of

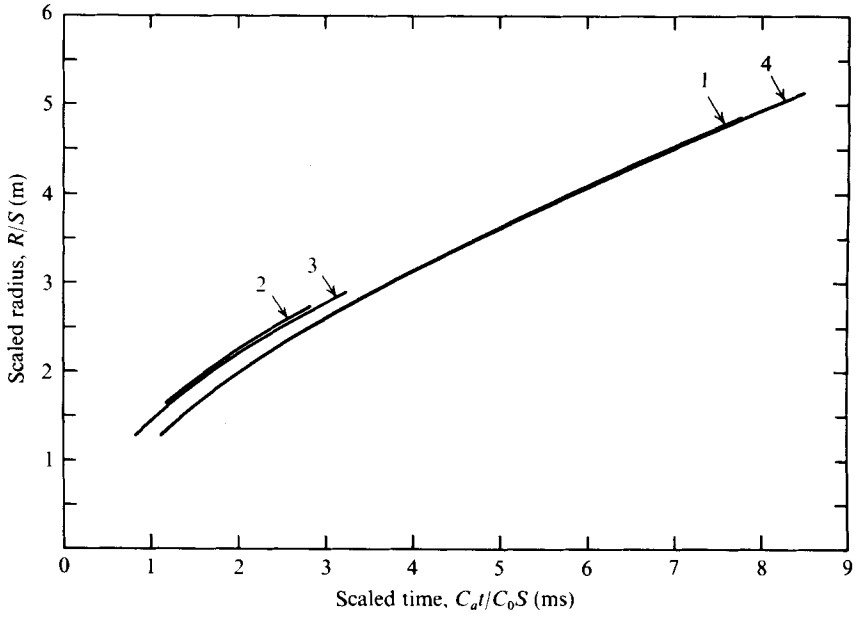

FIGURE 7. Scaled trajectories of the Mach stems beneath the ideal reflecting plane. The scaled distance of the charge centre from the interaction plane was 0·93 in experiments 1 and 4 and 0·57 m in experiments 2 and 3.

93·22 kPa and a relative humidity of 31 %, and experiment 4 at an ambient temperature of −19·1 °C, an atmospheric pressure of 94·34 kPa and a relative humidity of 60 %. The scaled trajectories are given in figure 6 (*b*), and show no significant difference between the two experiments.

The scaled trajectories of the primary shocks from the lower charge in each of the four experiments were essentially identical, indicating that all these charges detonated satisfactorily. It was not possible to obtain similar measurements for the four upper charges as their primary shocks were not visible against the backdrop, but it was assumed that the upper charges also detonated satisfactorily.

The scaled trajectories of the Mach-stem shocks below the ideal reflecting surfaces are shown in figure 7. Again, there is little difference between the trajectories of the shocks from the charges at the same distance from the interaction plane. The trajectories of the Mach-stem shocks above the ground are given in figure 8, and for each height of burst there is a significant difference between the trajectories above the smooth and rough ground. As might be expected, the shocks over the rough ground travelled more slowly than those over the smooth ground.

In figure 9 the overpressure ratio $P_s/P_0 - 1$ for the primary spherical shocks has been plotted against scaled distance from the charge centre. The results for experiments 1 and 4 are effectively identical. Single points only are plotted for experiments 2 and 3, in which the primary shock trajectories could be observed only for a distance of approximately 3 m. Results based on Brode's (1959) calculations are also shown, since they are known to give a good description of the variation with distance of the shock strength from a spherical charge of TNT. The slightly higher shock strength observed for the four experiments is undoubtedly due to the fact that 50 % PETN was used rather than pure TNT.

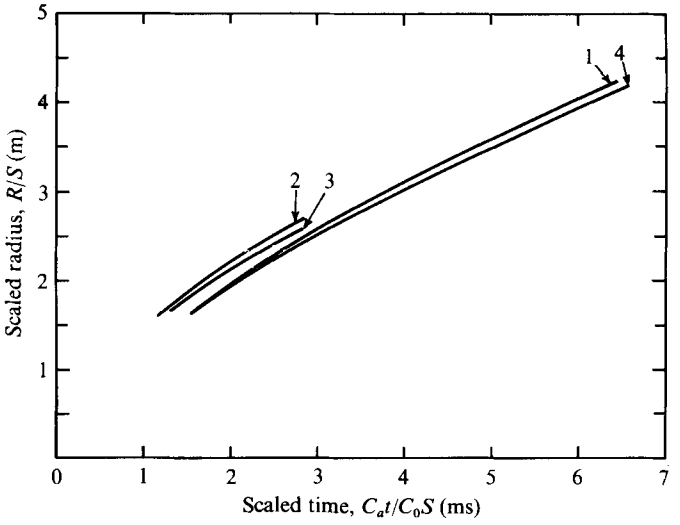

FIGURE 8. Trajectories of the Mach stems above the ground. The scaled height of the charge centre was 0·93 m in experiments 1 and 4 and 0·57 m in experiments 2 and 3.

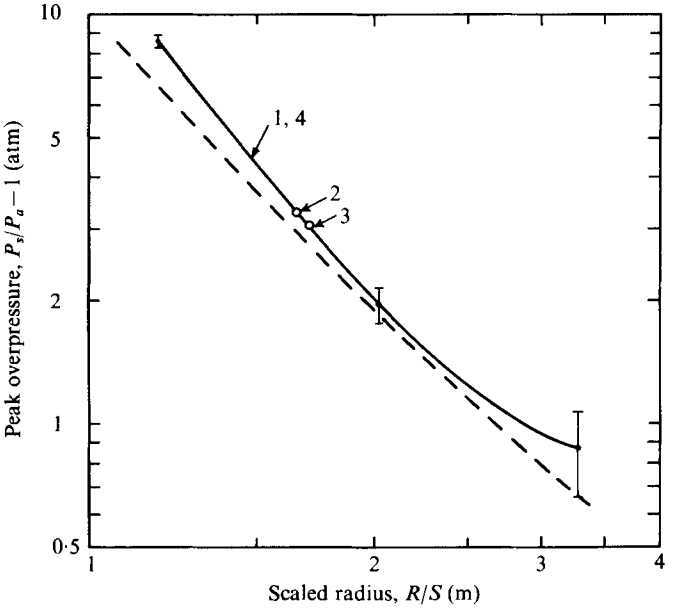

FIGURE 9. Strength (overpressure) of the primary shock fronts *vs.* distance. ○, measured values for the four pentolite explosions; ---, Brode's calculation for a TNT explosion. The error bars are estimates of the maximum accumulated error from all sources. The data scatter about the curves was approximately one-tenth of these values.

Figures 10(*a*) and (*b*) compare the strengths of the Mach-stem shocks along the ground with those along the ideal reflecting surface for each experiment. The shock strength is given in terms of the overpressure ratio and is plotted against the scaled distance from the axis of symmetry of each Mach stem. In each case the shock strength is higher along the ideal reflecting surface than along the ground, and the difference is much greater in the two experiments carried out over rough ground.

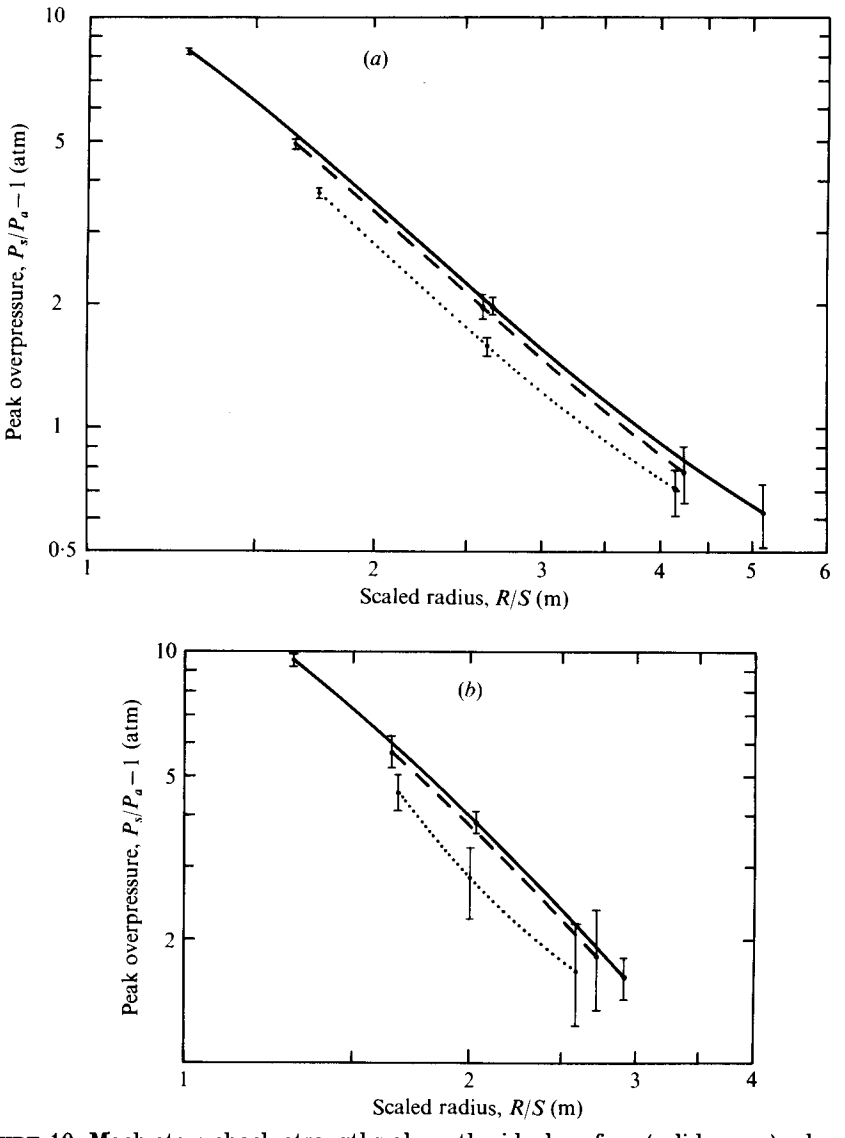

FIGURE 10. Mach-stem shock strengths along the ideal surface (solid curve), above the smooth ground (dashed curve) and above the rough ground (dotted curve) for a scaled height of the burst of (*a*) 0·93 m and (*b*) 0·57 m. The error bars are estimates of the maximum accumulated error from all sources.

Triple-point trajectories

The nature of the reflecting surface also had a significant effect on the triple-point trajectory. The loci of the triple points observed on experiments 1 and 4 are plotted in figure 11. The triple-point loci below the ideal reflecting surfaces were effectively identical in the two experiments. The effect of the ground surface was to lower the triple-point trajectory, the rough ground surface producing the more marked effect. The curves shown in figure 11 are best fits to the observed data points. In the cases of the triple-point loci produced at the ideal and smooth ground surfaces there was little scatter in the measured data, with an unscaled r.m.s. variation in height of 10 cm

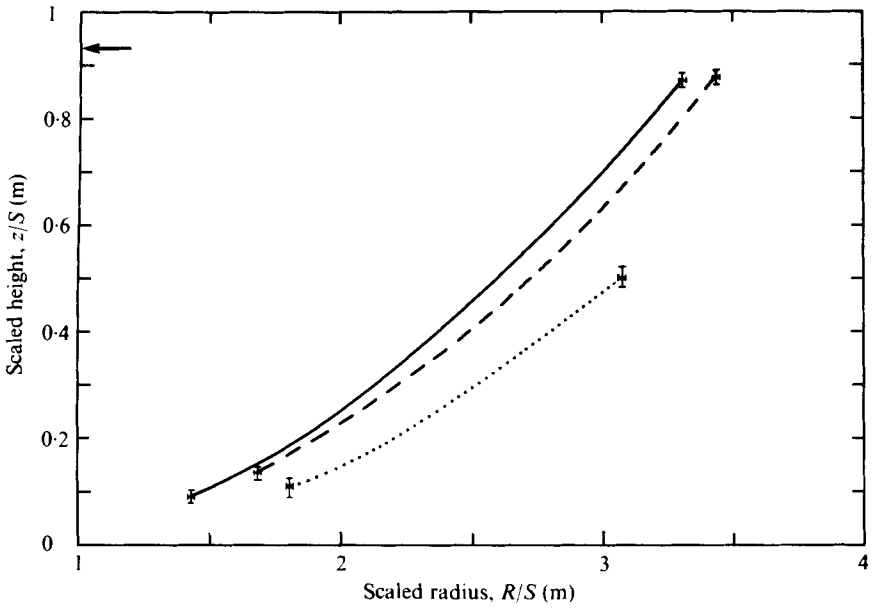

FIGURE 11. Loci of the triple points at the ideal surface (solid curve), over the smooth ground (dashed curve) and over the rough ground (dotted curve) for a scaled height of burst of 0·93 m. The error bars in this figure are the r.m.s. values of the data scatter about the curves.

about the fitted curve. However, in the case of the triple-point locus over the rough surface, there were significantly larger fluctuations in the height, with an unscaled r.m.s. variation of 16 cm. Over the rough ground surface the maximum variation of the triple-point height was approximately ± 35 cm, comparable to the scale of the ground roughness. The triple-point loci in experiments 2 and 3 showed similar qualitative effects but could be observed only for scaled distances of approximately 0·3 m.

5. Discussion

Magnitude of the effects produced by different reflecting surfaces

The experimental results illustrate differences in the Mach reflexion of spherical blast waves at real surfaces compared with an ideal surface. The effects are particularly noticeable over a rough as compared with a smooth surface. The nature of the reflecting surface affects both the strength of the Mach-stem shock and the locus of the triple point.

An attempt has been made to give a numerical value to the magnitude of the effects on the strength of the Mach-stem shock. The technique is based on that which has been used to compare the energy yields from different explosive sources, namely comparison of the cubes of the radii at which equal shock overpressures are observed. This is also the basis of the cube-root scaling law discussed earlier. For example, if a specific primary shock strength P_s/P_0 is measured at a radial distance R_1 from the centre of one symmetrical explosion and at a radial distance R_2 from the second such explosion, then the ratio of the energy yields of the two explosions is given by $(R_1/R_2)^3$. This ratio can be calculated for several shock strengths and the results averaged.

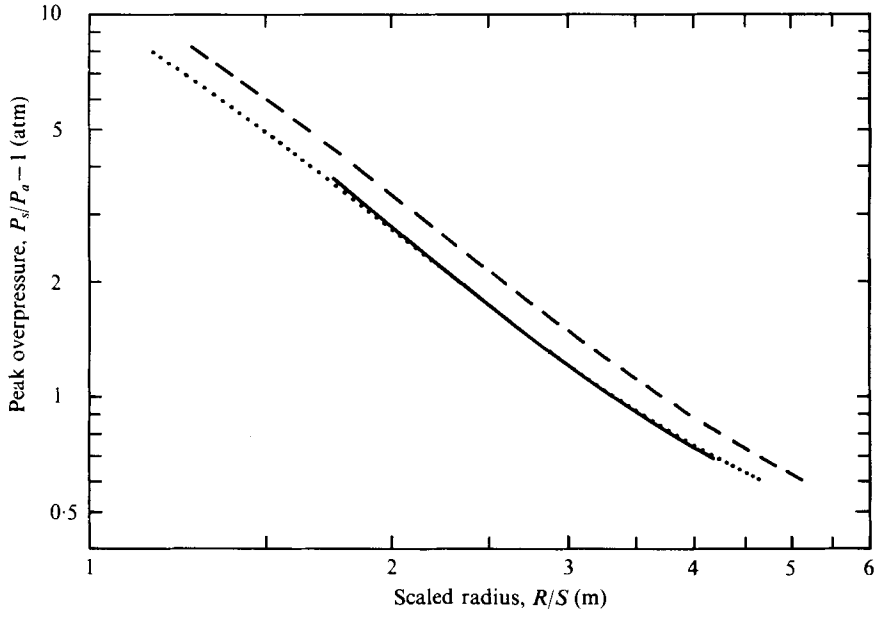

FIGURE 12. Shock strength *vs.* distance for the Mach stem over the rough ground (solid curve), the Mach stem along the ideal surface (dashed curve) and the Mach stem along the ideal surface scaled by an energy factor of 0·74 (dotted curve).

This technique was applied to obtain the results illustrated in figures 10(*a*) and (*b*), in which the shock overpressure–distance relationships are compared for the Mach-stem shocks over the ground and along the ideal reflecting surface. The cube of the ratio of the distances at which the same shock strength was observed for the two Mach stems was calculated at regular intervals of shock strength, and averaged. The average ratios in the experiments with the smooth ground surface were 0·86 ($\pm$ 0·04) and 0·93 ($\pm$ 0·02). The corresponding figures for the rough surface were both 0·74 ($\pm$ 0·03).

This is equivalent to stating that the Mach-stem shock over rough ground from a 1 kg explosion would be the same as that from a 0·74 kg explosion over an ideal reflecting surface. Such a comparison is made in figure 12, which shows the overpressure variation of the Mach stem along the ideal surface and over the rough ground, together with the ideal-surface results scaled by a factor of $(0{\cdot}74)^{\frac{1}{3}}$. The slight difference in the slopes of the two overlapping curves cannot be considered significant on the basis of these results, although intuitively one might expect a variation of the reflexion factor with shock strength, as reported for a shock produced by a hemispherical explosive charge on the ground surface compared with the spherical shock from a centred explosion (Dewey 1964). The fact that it is not possible to use a single-valued scaling factor to describe shock reflexions from real surfaces in terms of the reflexion from an ideal surface complicates the task of developing computer techniques to predict such phenomena. Any relationship between the reflexion factor and the shock strength is likely to be a complex one depending both on the physical properties of the reflecting medium and on the roughness of the solid–gas interface.

The energy calculations discussed above were based on the shock-front trajectories only, and it is not suggested that amounts of energy proportional to the differences in the scaling factors were transferred from the air blast waves to the ground surface.

The majority of the 'energy' not appearing at the shock front was undoubtedly redistributed within the blast wave and might be expected to appear in the form of extended pressure and kinetic energy profiles throughout the wave.

Energy distribution within the Mach-stem blast waves

The redistribution of energy within the blast waves as they passed over the ground was indicated by the transient pressure profiles measured with electronic transducers at ground level and at the level of the ideal reflecting surface. For example, transducers were placed at a distance of 18·3 m from the axes of symmetry in experiments 1 and 4. The ratios of the shock-front pressures measured by the transducers at ground level and at the level of the ideal reflecting plane were 0·84 and 0·79 respectively in the two experiments, representing a decrease of approximately 20 % in the shock strength at the ground compared with the ideal reflecting surface. In contrast, the corresponding ratios of the measured pressure impulses, defined as the pressure–time integral up to the time at which the pressure first returned to the ambient value, were 1·17 and 1·11 respectively, indicating an increase in the positive impulse of approximately 15 % over the ground compared with the ideal surface. Qualitatively similar results were obtained from other pairs of pressure transducers at various distances from the axes of symmetry and in the other two experiments.

In order to study the complete energy profile throughout a blast wave it would be necessary to know, independently, the pressure, density and particle velocity profiles. The pressure profiles were measured by electronic transducers at a number of positions, and in addition it is hoped that it will be possible to obtain density and particle velocity profiles from an analysis of the photographically observed particle trajectories, which was a separate project in these experiments, to be reported later.

6. Conclusions

A successful technique has been developed for observing the interaction of two identical large-scale spherical blast waves. Since this interaction occurs without loss of energy, the resulting Mach-stem blast wave can be considered as that produced by an ideal reflexion, in which no energy is absorbed or redistributed by the reflecting medium. The two explosions in each of the four experiments were simultaneous to within a few microseconds, and although it was not possible to measure the primary blast waves from the upper charges, there was no observable lack of symmetry in any experiment, so that it could be assumed that all the explosions were of the same energy yield. Previous attempts to produce simultaneous explosions of equal energy yield were not entirely successful owing to inaccuracies in initiation of detonation and variations in the detonation efficiency of TNT. It was for the latter reason that Pentolite was used in these experiments.

High-speed photogrammetrical techniques which had been developed for studying single explosions were successfully modified for the double-explosion experiments so that simultaneous observations could be made of the ideal Mach stem and the Mach stem over the ground. Two types of ground surface, smooth and rough, and two heights of burst were used in the four experiments.

Photogrammetry of the Mach-stem shock fronts gave an accurate determination of the time-resolved shock trajectories from which the spatial variation of shock

strength could be obtained. Significant differences were observed in the Mach shock strengths and triple-point trajectories over the ground compared with those along the ideal reflexion plane. In terms of energy scaling these differences in shock strength were as large as 10 % and 25 % over the smooth and rough ground surfaces respectively. The paths of the triple points over the ground were lower than over the ideal plane. In the region in which the triple-point trajectory could be observed its heights over the smooth and rough ground respectively were, on the average, $0{\cdot}91 \pm 0{\cdot}02$ and $0{\cdot}64 \pm 0{\cdot}04$ of the distance from the ideal reflecting surface.

The results reported here will be used for the evaluation of computer codes designed to simulate shock and blast wave reflexions. Further experimental studies are being carried out to determine the energy distribution within reflected blast waves, so that appropriate methods can be devised to account for energy absorption and redistribution in computer simulations of blast reflexions.

The authors gratefully acknowledge the opportunity offered by the Defence Research Establishment Suffield and the Defence Nuclear Agency to participate in the experiments described in this paper. The analyses were carried out with the assistance of a contract from the Canadian General Electric Company, and with additional financial support by the Defence Research Board and the National Research Council of Canada. The advice and assistance of A. P. R. Lambert and J. Keefer are gratefully acknowledged.

REFERENCES

Amsden, A. & Hirt, C. W. 1973 *Los Alamos Rep.* LA-5100.
Brode, H. L. 1959 *Phys. Fluids* **2**, 217.
Dewey, J. M. 1964 *Proc. Roy. Soc.* A **279**, 366.
Dewey, J. M. 1971 *Proc. Roy. Soc.* A **324**, 275.
Dewey, J. M. & Walker, D. K. 1975 *J. Appl. Phys.* **46**, 3454.
Henderson, L. F. & Lozzi, A. 1975 *J. Fluid Mech.* **68**, 139.